ISSN 1674-1056
http://cpb.iphy.ac.cn
http://iopscience.iop.org/cpb
中国物理 B
Chinese Physics
中国物理 Chinese Physics B

Enhancement of MAD/MIR phasing at low resolution and a new procedure for automatic phase extension

Pu Han(韩普)[1,2], Yuan-Xin Gu(古元新)[1], Wei Ding(丁玮)[1], Hai-Fu Fan(范海福)[1]

Citation: Chin. Phys. B . 2019, 28(7): 076108. **doi:** 10.1088/1674-1056/28/7/076108
Journal homepage: http://cpb.iphy.ac.cn; http://iopscience.iop.org/cpb

What follows is a list of articles you may be interested in

Effects of helium irradiation dose and temperature on the damage evolution of Ti_3SiC_2 ceramic

Hua-Hai Shen(申华海), Xia Xiang(向霞), Hai-Bin Zhang(张海斌), Xiao-Song Zhou(周晓松), Hong-Xiang Deng(邓洪祥), Xiao-Tao Zu(祖小涛)

Chin. Phys. B . 2019, 28(7): 076104. **doi:** 10.1088/1674-1056/28/7/076104

Microstructure and lateral conductivity control of hydrogenated nanocrystalline silicon oxide and its application in a-Si:H/a-SiGe:H tandem solar cells

Tian-Tian Li(李天天), Tie Yang(杨铁), Jia Fang(方家), De-Kun Zhang(张德坤), Jian Sun(孙建), Chang-Chun Wei(魏长春), Sheng-Zhi Xu(许盛之), Guang-Cai Wang(王广才), Cai-Chi Liu(刘彩池), Ying Zhao(赵颖), Xiao-Dan Zhang(张晓丹)

Chin. Phys. B . 2016, 25(4): 046101. **doi:** 10.1088/1674-1056/25/4/046101

FT-Raman spectroscopy study of solvent-in-salt electrolytes

Liumin Suo(索鎏敏), Zheng Fang(方铮), Yong-Sheng Hu(胡勇胜), Liquan Chen(陈立泉)

Chin. Phys. B . 2016, 25(1): 016101. **doi:** 10.1088/1674-1056/25/1/016101

Complementary method to locate atomic coordinates by combined searching method of structure-sensitive indexes based on bond valence method

Song Zhen, Liu Xiao-Lang, He Li-Zhu, Xia Zhi-Guo, Liu Quan-Lin

Chin. Phys. B . 2015, 24(10): 106101. **doi:** 10.1088/1674-1056/24/10/106101

Enhancement of MAD/MIR phasing at low resolution and a new procedure for automatic phase extension*

Pu Han(韩普)[1,2], Yuan-Xin Gu(古元新)[1], Wei Ding(丁玮)[1,†], and Hai-Fu Fan(范海福)[1,‡]

[1] *Key Laboratory of Soft Matter Physics, Institute of Physics, Chinese Academy of Sciences, Beijing* 100190, *China*
[2] *School of Physics Science, University of Chinese Academy of Sciences, Beijing* 100049, *China*

(Received 5 May 2019; revised manuscript received 20 May 2019; published online 25 June 2019)

To achieve *de novo* protein structure determination of challenging cases, multi-wavelength anomalous diffraction (MAD) and multiple isomorphous replacement (MIR) phasing can be powerful tools to obtain low-resolution initial phases from heavy-atom derivative datasets, then phase extension is needed against high-resolution data to obtain accurate structures. In this context, we propose a direct-methods procedure here that could improve the initial low-resolution MAD/MIR phase quality. And accordingly, an automated process for extending initial phases to high resolution is also described. These two procedures are both implanted in the newly released IPCAS pipeline. Three cases are used to perform the test, including one set of 4.17 Å MAD data from a membrane protein and two sets of MAD/MIR data with derivatives truncated down to 6.80 Å and 6.90 Å, respectively. All the results have shown that the initial phases generated from the direct-methods procedure are better than that from the conventional MAD/MIR methods. The automated phase extensions for the latter two cases starting from 6.80 Å to 3.00 Å and 6.90 Å to 2.80 Å are proved to be successful, leading to complete models. This may provide convenient and reliable tools for phase improvement and phase extension in difficult low-resolution tasks.

Keywords: direct methods, multi-wavelength anomalous diffraction (MAD)/multiple isomorphous replacement (MIR) phasing, phase extension, low-resolution

PACS: 61.05.–a **DOI:** 10.1088/1674-1056/28/7/076108

1. Introduction

Experimental phasing methods are the major choices for *de novo* protein structure determinations in x-ray crystallography. In these methods, phasing process starts with finding the substructures in the asymmetric unit of derivative crystals and the initial phases are calculated via different types of techniques, such as single-wavelength anomalous diffraction (SAD), single isomorphous replacement (SIR), multi-wavelength anomalous diffraction (MAD), multiple isomorphous replacement (MIR), SIR with anomalous scattering (SIRAS), and MIR with anomalous scattering (MIRAS).[1] As the phase ambiguity is intrinsic in SAD/SIR, the MAD/MIR phasing is more powerful for combining the bimodal phase distribution of several SAD/SIR data sets to give the unique phase indication for each individual reflection. Programs such as SHARP, SOLVE, and MLPHARE are all available to obtain the phase information via conventional MAD/MIR methods.[2–4] In some challenging cases of membrane proteins or large complexes, the intrinsic disorder or flexibility often results in low resolution[5] (say about 6.00 Å lower) in the heavy-atom derivative data, making it difficult for crystallographers to obtain the initial phases. Even under this condition, MAD and MIR are still reliable and can provide useful information for the structure determination.

However, MAD and MIR have their own limitations: for MIR, the isomorphism between the native and the derivatives is not always perfect; for MAD, the severe radiation damages may lead to weak anomalous signals in the individual SAD data sets. These problems can be even serious when dealing with cases from poorly diffracted crystals, making the phases interpretation ambiguous in high-resolution and the good-quality phases only available at lower resolution.[6] Therefore, we propose here an iterative direct-methods MAD/MIR phasing procedure in order to eliminate the effects of these problems. It integrates the iterative direct-methods SAD/SIR phasing[7,8] with the conventional MAD/MIR methods and testing results with three cases at low resolution have shown this hybrid-procedure is better than using single method alone.

During our test, we find that the resulting low-resolution initial phases obtained by the hybrid procedure mentioned above are far from sufficient to generate an interpretable electron density map from either manual or automated model building. Phase extension is therefore becoming an essential part in the following process. In addition, prior knowledge of the structure such as the non-crystallographic symmetry (NCS), homologous template, or multi-crystal information is often needed in difficult phase extension cases.[9,10] And when the prior structure knowledge is unavailable, the automated phase extension would become a grand challenge.

There are many different methods for conducting the

*Project supported by the National Basic Research Program of China (Grant No. 2011CB911100) of the Ministry of Science and Technology of China.
†Corresponding author. E-mail: dingwei@iphy.ac.cn
‡Corresponding author. E-mail: fan@iphy.ac.cn
© 2019 Chinese Physical Society and IOP Publishing Ltd

phase extension procedure, such as the solvent-flattening,[11] histogram matching,[12] the maximum-entropy method,[13] and the maximum likelihood density modification.[14] In practice, all the methods above were incorporated with the solvent-flattening technique within a dual-space framework to improve their own efficiency. We present here an iterative direct-methods phase extension procedure by modifying the iterative direct-methods-aided partial-model extension proposed in 2007.[15] This method differs from all the above in that it uses direct methods to provide phase constraint in the reciprocal space and, in addition, it is independent of prior structure knowledge. Two testing cases with starting phases at 6.90 Å and 6.80 Å have been successfully extended to native data at resolutions of 2.80 Å and 3.00 Å, respectively, and the final resulting models agree well with the previous entry structures in Protein Data Bank (PDB; http://www.pdb.org/).

2. Methods

The method consists of two stages, the first stage is to obtain the low-resolution initial phases via a direct-methods MAD/MIR phasing procedure, while the second stage is to extend the low-resolution phases to higher resolution automatically. The details of these two stages will be described in the following sections.

2.1. Stage 1: iterative direct-methods MAD/MIR phasing procedure

This procedure is featured as follows.

(i) Phases are first calculated by the conventional MAD/MIR methods;

(ii) MAD/MIR phases from step (i) are cut off to low resolution and used as the starting "known phases" for the direct-methods SAD/SIR phasing. For details of direct methods SAD/SIR phasing, please refer to Refs. [7] and [8].

(iii) Among the MAD/MIR derivative datasets, one set with the strongest anomalous signal or the highest resolution is selected to conduct the iterative direct-methods SAD/SIR phasing based on the starting known phases from step (ii).

(iv) Each cycle of the procedures consists of three parts: direct method phasing, density modification, and model building/refinement. Starting from the second cycle onwards, models from last cycle will be fed back to the current cycle. The known phases will be "fixed" in each cycle until the percentage of residues built has reached certain standard that users define (say about 80%).

In practice, SAD/SIR phase estimations are not as accurate as MAD/MIR because of the intrinsic phase ambiguity, while the direct-methods proposed by Fan and Gu[16] in 1985 was designed to overcome this problem by changing the 0–2π phase problem into making a choice between the sign of plus and minus. In addition, with the help of those high-quality and low-resolution known phases as starting point, the $P+$ formula deduced from this theory[16] will give a more accurate modulation to the bimodal phase probability distribution, thus strengthening the phasing power. The "fixed" in step (iv) means the known phases remain unchanged in the direct-methods phase calculation, and these phases are used to calculate the value of $P+$ instead of setting it to a constant value of 0.5. Please refer to Ref. [6] for more details.

So as it is, the procedure has achieved two things at one stock. The starting known phases from the MAD/MIR procedure at low resolution can greatly enhance the phasing power of direct methods, while the low-resolution MAD/MIR phases can be extended to higher resolution with the aid of SAD/SIR iteration. What is more, by choosing only one set of derivative data with strongest anomalous signal or highest resolution, the phasing result would be less affected by the imperfect isomorphism or the weak anomalous signals. The high-resolution derivative data will not be limited by other low-resolution datasets and can be used to its full potential.

The flowchart of the iterative direct-methods MAD/MIR phasing procedure is presented in Fig. 1. Programs in charge of this procedure are OASIS for direct method phasing, DM[17] for density modification, and AutoBuild[18] for the model building and refinement.

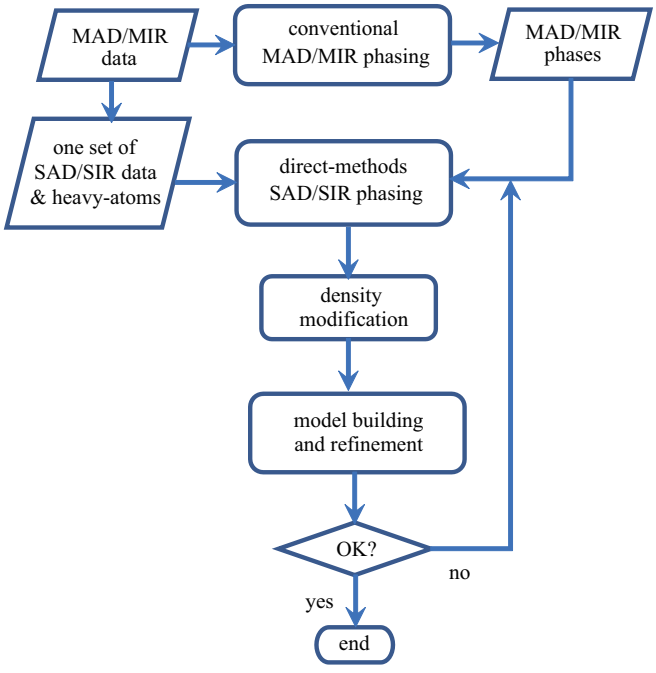


Fig. 1. Flowchart of the iterative direct-methods MAD/MIR phasing.

2.2. Stage 2: iterative direct-methods phase extension

This procedure was originally proposed in 2007 as a direct-methods-aided partial-model extension without the needs of SAD/SIR information. By redefining the variables in the $P+$ probability formula proposed by Fan and Gu,[16] the

phase extension process of finding a value in the range of 0–2π for each unknown phase is reduced into that of just making a choice between two possible values. It is more like a "phase-flipping" process, where the phases that differ much from the correct value will undergo a large shift, while the phases that are close to the correct value will remain unchanged. For more details, please refer to Ref. [15].

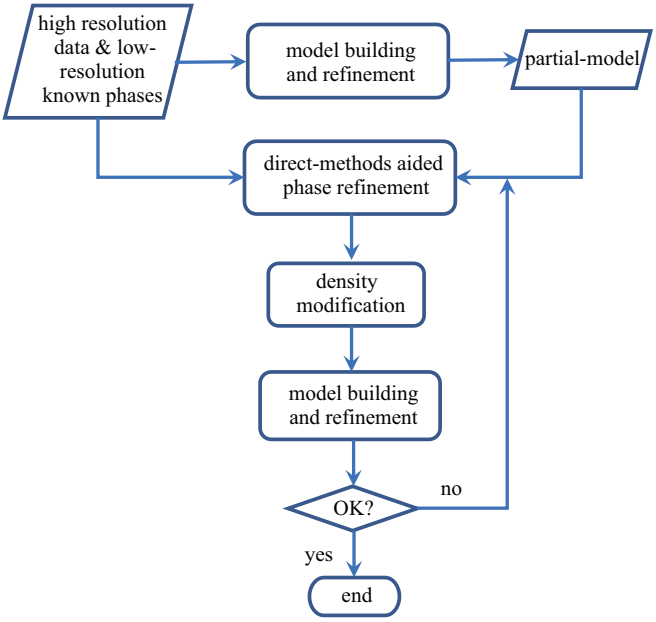


Fig. 2. Flowchart of the iterative direct-methods phase extension.

Usually, the direct-methods-aided partial-model extension starts with an incomplete model. However, the density map calculated at low resolution from stage 1 may not be sufficient enough to build a reliable structural model, so we first use the initial phases to build up a model against the structure amplitudes with high-resolution. Then the resulting initial model will be the starting information for the direct methods phasing in OASIS. At the same time, the initial phases can also be used as "known phases" that remain fixed in the iteration until the resultant model has grown to the standard defined by users (say about 80% of the whole structure).

The flowchart of the iterative direct-methods phase extension procedure is displayed in Fig. 2. Programs involved in this procedure are AutoBuild for the initial model building, OASIS for the direct method phasing, DM for the density modification, and AutoBuild and Buccaneer[19] for the model building and refinement.

3. Testing and results

All the tests stated in this section are conducted in the newly released IPCAS 2.0 pipeline. The programs and their usage in the tests are listed in Table 1. The details of the testing processes are described as follows.

Table 1. Programs used in the test.

Program	Version	Usage
AutoBuild	PHENIX 1.15.2	model building/refinement
DM	version 7.0 in CCP4 7.0.073	density modification
OASIS	version 4.2 in IPCAS 2.0	direct-methods phasing
Buccaneer	version 1.6.5 in CCP4 7.0.073	model building
REFMAC	version 5.8 in CCP4 7.0.073	structure refinement
RESOLVE	PHENIX 1.15.2	iterative density modification for phase extension
SOLVE	PHENIX 1.15.2	MIR phasing
SHARP	version 2.8	MAD phasing

3.1. Testing data sets

Three sets of protein data are used to test the methods, including the MAD data of the human K2P TRAAK channel

Table 2. Crystallographic statistics of testing cases.

	The human K2P TRAAK channel			Human BK channel Ca^{2+} gating apparatus				R-phycoerythrin				
PDB code	3UM7			3MT5				1LIA				
No. of residues in the AU	618			726				668				
NCS copies	2			1				2				
Data	Native	Derivative (peak)	Derivative (inflection)	Native	Derivative (peak)	Derivative (inflection)	Derivative (remote)	Native	Derivative	Derivative	Derivative	Derivative
Resolution	3.30 × 3.80 × 3.80[a]	4.17	4.17	3.00	3.30 (6.80[b])	3.30 (6.80[b])	3.30 (6.80[b])	2.80	5.00 (6.90[b])	4.50 (6.90[b])	4.00 (6.90[b])	3.00 (6.90[b])
Heavy-atom sites	/	Tl (7)	Tl (7)	/	Se (13)	Se (13)	Se (13)	/	Hg	Hg	Pt	Au
Bijveot ratio/%	/	8.20	8.21	/	3.92	3.91	3.78	/	/	/	/	/
Space group	$P2_12_12_1$	$P2_12_12_1$		$P6_322$	$P6_322$	$P6_322$	$P6_322$	$R3$	$R3$	$R3$	$R3$	$R3$
Unit cell a/Å	87.9	87.5		144.5		145.1		189.8		189.8		
Unit cell b/Å	130.9	130.7		144.5		145.1		189.8		189.8		
Unit cell c/Å	132.8	132.1		182.2		182.4		60.1		60.1		
Unit cell α/(°)	90	90		90		90		90		90		
Unit cell β/(°)	90	90		90		90		90		90		
Unit cell γ/(°)	90	90		120		120		120		120		
Wavelength/Å	0.9783	0.9783	0.9791	0.9792	0.9792	0.9793	0.9640			/		
R_{merge}/%	/	/	/	8.9 (73.8)	10.5 (49.3)	10.0(53.3)	13.0(74.5)			/		
I/σ_I	25.6(1.4)	15.6(1.3)	14.2(1.1)	19.6 (2.4)	18.8 (3.3)	18.2(3.1)	13.9(2.2)			/		
Completeness/%	73.4(4.9)	98.2(99.3)	98.4(99.3)	99.9 (99.9)	99.8 (100.0)	99.8(100.0)	99.8(100.0)			/		
Redundancy	3.7(4.5)	3.6(3.7)	3.6(3.7)	5.8 (5.9)	7.0 (7.2)	7.0 (7.2)	7.0 (7.2)			/		

[a]Native data were anisotropically truncated to 3.30 × 3.80 × 3.80 Å prior to scaling.
[b]The resolution of the truncated data.
In the row of "R_{merge}", "I/σ_I", "Completeness", and "Redundancy", the numbers in parentheses represent values in the highest-resolution shell.

(PDB_ID: 3UM7),[20] the MAD data of the human BK channel Ca^{2+} gating apparatus (PDB_ID: 3MT5),[21] and the MIR data of the R-phycoerythrin (PDB_ID: 1LIA).[22] In addition, the derivative data sets of 3MT5 and 1LIA are manually truncated to 6.80 Å (original resolution: 3.30 Å) and 6.90 Å (original resolution: 3.00 Å). For all the three cases above, we use the previously deposited model in the PDB as the reference model in our test. Detailed data statistics are listed in Table 2.

3.2. MAD and MIR phasing

The human K2P TRAAK channel (3UM7) is a membrane protein. In the original work, the initial phases were calculated in SHARP via MIRAS method and the final model was built by iterative manual building.

During the test, the conventional MAD phases and heavy-atoms are firstly calculated by SHARP, then the MAD phases are truncated to 8.00 Å and regarded as the "known phases". The diffraction data from the "peak" wavelength at 4.17 Å resolution along with the known phases are used to conduct the direct-methods MAD phasing for 20 cycles of iteration (IPCAS iteration control: OASIS+DM+AutoBuild). The resulting electron density matches well with the reference model (see Fig. 3(a)) and the backbone structure auto traced from the density map covers 51.2% of the total residues.

The human BK channel Ca^{2+} gating apparatus is also a membrane protein. In the original work, initial phases were calculated by MAD phasing and the model was generated and extended against native data by iterative manual building.

In the testing case, the heavy-atoms and MAD phases are firstly calculated by SHARP, then the MAD phases are truncated to 8.00 Å and regarded as the "known phases". The truncated 6.80 Å "peak-wavelength" data along with the known phases are used to conduct the iterative direct-methods MAD phasing for 20 cycles of iteration (IPCAS iteration control: OASIS+AutoBuild). Finally, a backbone-structure has been generated with 41.8% of the total residues built from the resulting density map. The map matches reasonably with the reference model (see Fig. 3(b)).

The structure of R-phycoerythrin (Rpe) was originally determined via MIR method with four sets of derivative data and the native data.

In our test, the heavy-atoms and the conventional MIR phases are firstly calculated by SOLVE.[3] Then the MIR phases are truncated to 8.00 Å resolution and regarded as the "known phases". The truncated 6.90 Å Au-derivative data and the native data along with the initial known phases are used to conduct the iterative direct-methods MIR phasing for 20 cycles of iteration (IPCAS iteration control: OASIS+AutoBuild). 71.2% of the total residues are auto traced by the resulting electron density map which has revealed the essential features of the reference model (see Fig. 3(c)).

For all the three testing cases above, we have compared the final figure-of-merit (FOM)-weighted mean phase error of the conventional MAD/MIR phasing, the iterative direct-methods SAD/SIR phasing, and the iterative direct-methods MAD/MIR phasing, respectively. The results of the iterative direct-methods MAD/MIR phasing are evidently better than the other two phasing methods, proving that it could further improve the conventional MAD/MIR phases. Detailed resulting information is listed in Table 3.

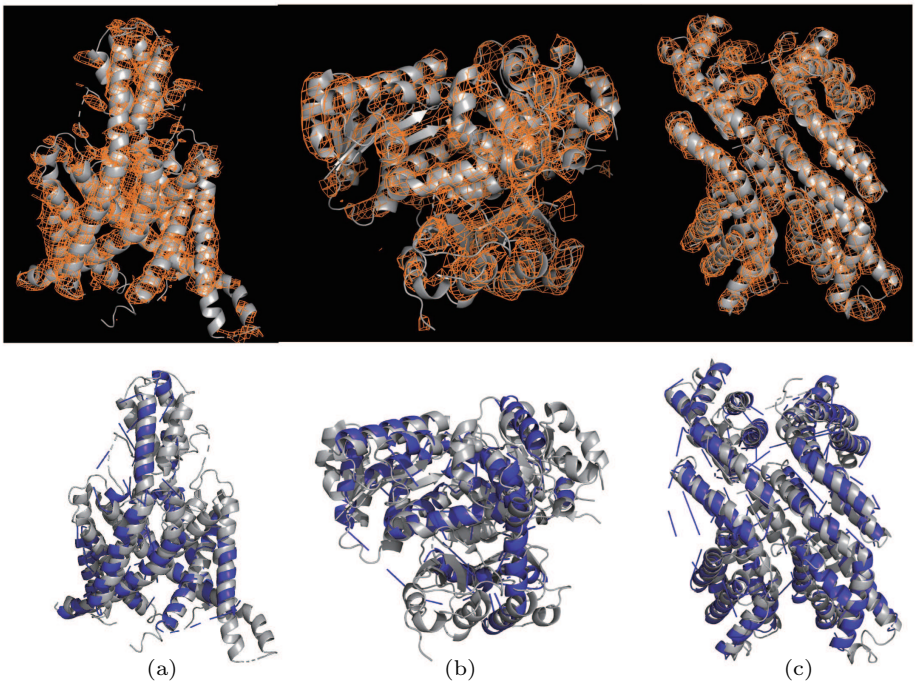


Fig. 3. Results of three cases from stage 1: (a) 3UM7; (b) 3MT5; (c) 1LIA. The upper part represents the resulting electron density maps (the orange meshes) contoured at 1.5 σ, and the reference models are shown in gray cartoons. The bottom part shows the resulting models (blue) superimposed with the corresponding reference models (grey). This figure is made by PyMOL.[23]

Table 3. Results for three testing cases in stage 1.

Protein	PDB-ID	Reference model length[a]	Direct-methods MAD/MIR phasing				FOM weighted mean phase error of different phasing methods/(°)		
			Resolution/Å	R_{work}/R_{free}	Residues built/%[b]	CPU times (h:min:s)	Direct-methods MAD/MIR phasing	Direct-methods SAD/SIR phasing	MAD/MIR phasing
The human K2P TRAAK channel	3UM7	503	4.17	0.47/0.48	51.2	01:37:20	70.88	86.00	78.78
Human BK channel Ca^{2+} gating apparatus	3MT5	593	6.80	0.49/0.53	41.8	02:10:34	35.44	69.74	40.28
R-phycoerythrin (Rpe)	1LIA	668	6.90	0.42/0.45	71.2	00:50:53	37.97	62.01	51.20

[a]Total residue number of the reference model.

[b]Number of residues in the model built by the model-building programs.

3.3. Phase extension

Although the "sausage-like" electron density maps obtained in stage 1 have revealed some basic characteristics of the structure, the models are lack of accurate side-chain information owing to the low resolution of the diffraction data. In order to obtain more precise structures, the phase extension is conducted.

In the human K2P TRAAK channel case, we have failed to automatically extend the phase and model to higher resolution owing to the severe anisotropy displayed in the native data which is elliptically truncated and scaled to $3.80 \times 3.30 \times 3.80$ Å. While for the other two cases, automated phase extensions are successfully achieved.

For the human BK channel Ca^{2+} gating apparatus case, the 6.80 Å phases from stage 1 are firstly used to build an initial model and refined by PHENIX.AutoBuild against the 3.00 Å native data. Then the model as well as the native data is used to conduct the direct-method phase extension for 17 cycles of iteration. The final model is nearly completed with R_{work}/R_{free} reaching 0.25/0.29. The results of cycles 0, 4, 10, and 17 are listed in Table 4, and the models of cycles 0, 4, and 17 are shown in Fig. 4. The electron density maps are figured by COOT[24] to show the successful phase extension from 6.80 Å to 3.00 Å resolution (see Fig. 6(a)). As there is no NCS information within the unit cell, the testing result proves that the direct-methods phase extension procedure could be independent of the aid of the prior NCS information in the challenging case.

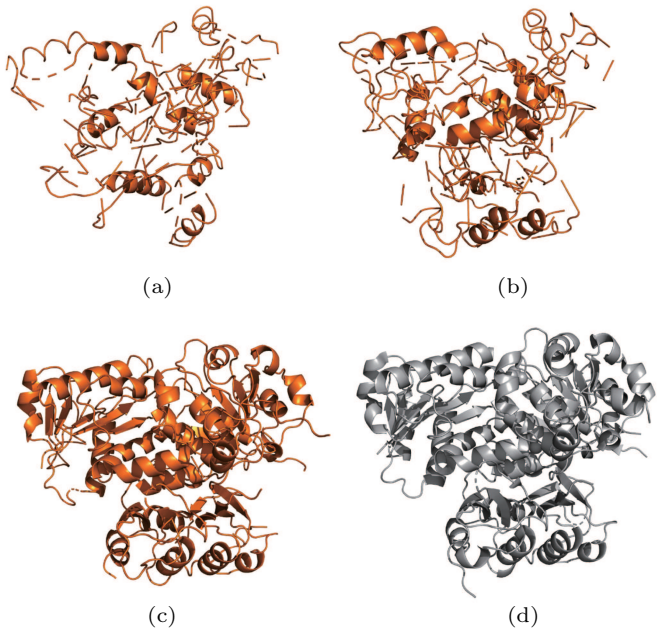


Fig. 4. Results of iterative direct-methods phase extension of 3MT5 (from 6.80 Å initial phases to 3.00 Å structure): (a) model from cycle 0; (b) model from cycle 4; (c) model from cycle 17; (d) the reference model.

Table 4. Results of low-resolution phase extension for 3MT5 in stage 2.

Cycle	FOM-weighted mean phase error/(°)	R_{work}/R_{free}	Number of residues built[b]	Number of residues placed[c]	No. of Cα with $\Delta C\alpha^a \leq 1.00$ Å	Cα-atom RMSD/Å
0	63.40	0.50/0.54	242	5	71	2.85
4	48.56	0.46/0.52	364	32	93	2.26
10	29.64	0.41/0.49	401	81	226	1.69
17	23.72	0.25/0.29	602	583	544	0.94
AutoBuild	82.79	0.46/0.52	307	26	13	2.88

[a]ΔCα is the deviation of Cα atoms between the resulting final model and the reference model.

[b]The number of residues in the model built by model-building programs.

[c]The number of residues that match the sequence.

The case of 1LIA has a two-fold NCS operator. The 6.90 Å phases are firstly used to build an initial model and refined by PHENIX.AutoBuild against the 2.80 Å native data. Then the model as well as the native data is used to conduct the direct-method phase extension for 15 cycles of iteration. The final model is nearly completed with $R_{\rm work}/R_{\rm free}$ reaching 0.25/0.28. The results of cycles 0, 4, 8, and 15 are listed in Table 5 and the models of cycles 0, 4, and 15 are shown in Fig. 5. The electron density maps from 6.90 Å to 2.80 Å resolution are displayed in COOT (see Fig. 6(b)).

We have made a comparison in phase extension between RESOLVE[25] in PHENIX with our direct-methods phase extension procedure. The phases after extension in RESOLVE are then delivered to PHENIX.AutoBuild for model building and refinement, and the building results of the two cases are listed in Tables 4 and 5, respectively. We can see that RESOLVE has failed in extending phases good enough for automatic model building while the direct-methods phase extension has achieved.

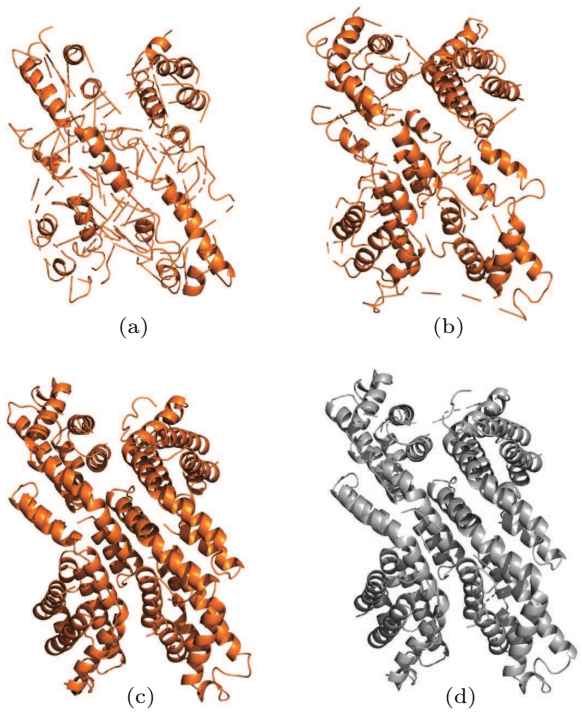


Fig. 5. Results of iterative direct-methods phase extension of 1LIA (from 6.90 Å initial phases to 2.80 Å structure): (a) model from cycle 0; (b) model from cycle 4; (c) model from cycle 15; (d) the reference model.

Table 5. Results of low-resolution phase extension for 1LIA in stage 2.

Cycle	FOM-weighted mean phase error/(°)	$R_{\rm work}/R_{\rm free}$	Number of residues built[b]	Number of residues placed[c]	No. of Cα with ΔCα[a] $\leq$ 1.00 Å	Cα-atom RMSD/Å
0	70.62	0.42/0.48	359	17	161	1.45
4	50.23	0.37/0.44	429	28	294	1.69
8	38.11	0.32/0.42	532	294	452	1.04
15	31.08	0.25/0.28	684	677	644	0.87
AutoBuild	79.92	0.39/0.46	360	69	51	2.01

[a]ΔCα is the deviation of Cα atoms between the resulting final model and the reference model.

[b]The number of residues in the model built by model-building programs.

[c]The number of residues that match the sequence.

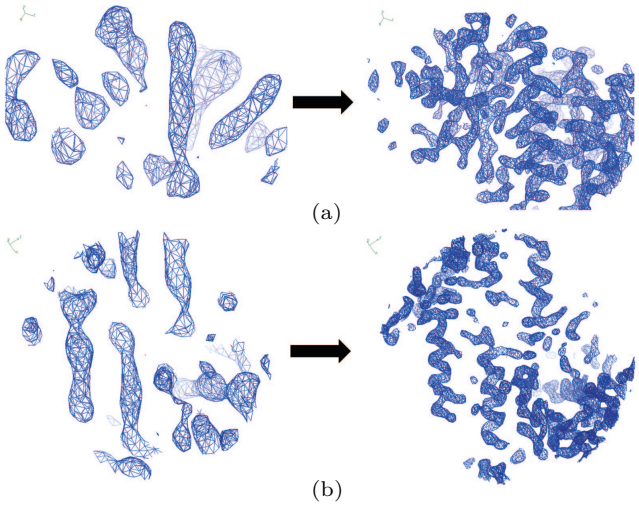


Fig. 6. Electron density maps before (left column) and after (right column) the iterative direct-methods phase extension: (a) 6.80 Å map extends to 3.00 Å map for 3MT5; (b) 6.90 Å map extends to 2.80 Å map for 1LIA. This figure is made in COOT.

4. Conclusion and perspectives

The iterative direct-methods MAD/MIR phasing procedure is proved to be reliable to improve the phase quality calculated from the conventional MAD/MIR methods at low resolution. The iterative direct-methods phase extension procedure is capable of extending phases automatically in two specific cases (case from 6.90 Å to 2.80 Å and case from 6.80 Å to 3.00 Å), both resulting in nearly completed models. The techniques proposed in this paper are useful and reliable when dealing with MAD/MIR data with derivative crystals diffracting to much lower resolution and native crystal diffracting to high resolution.

Furthermore, low-resolution phases from other sources such as molecular replacement (MR) template, cryoEM map, or even nuclear magnetic resonance (NMR) data can be possibly extended to high resolution by using the procedure described in this article. In addition, as the success of the direct-

methods phase extension depends on the quality of the initial phases and the resolution of the high-resolution data, quantitative analysis is needed to investigate how these factors influence the final results. By accomplishing this, more applications in protein crystallography will be discovered via this low-resolution phase extension tool.

Acknowledgment

The authors would like to thank Professor D. C. Liang for the data courtesy of 1LIA.

References

[1] McCoy A J and Read R J 2010 *Acta Cryst. D* **66** 458
[2] De La Fortelle E and Bricogne G 1997 *Methods Enzymol.* **276** 472
[3] Terwilliger T C and Berendzen J 1999 *Acta Cryst. D* **55** 849
[4] Winn M D, Ballard C C, Cowtan K D, Dodson E J, Emsley P, Evans P R, Keegan R M, Krissinel E B, Leslie A G W, McCoy A, McNicholas S J, Murshudov G N, Pannu N S, Potterton E A, Powell H R, Read R J, Vagin A and Wilson K S 2011 *Acta Cryst. D* **67** 235
[5] Brunger A T, DeLaBarre B, Davies J M and Weis W I 2009 *Acta Cryst. D* **65** 128
[6] Zheng X F, Zheng C D, Gu Y X, Mo Y D, Fan H F and Hao Q 1997 *Acta Cryst. D* **53** 49
[7] Wang J, Chen J, Gu Y, Zheng C and Fan H 2004 *Acta Cryst. D* **60** 1991
[8] Wang J, Chen J, Gu Y, Zheng C, Jiang F and Fan H 2004 *Acta Cryst. D* **60** 1987
[9] Pedersen B P, Morth J P and Nissen P 2010 *Acta Cryst. D* **66** 309
[10] Van Rooyen J M, Abratt Valerie R, Belrhali H and Sewell T 2011 *Structure* **19** 471
[11] Wang B C 1985 *Methods Enzymol.* **115** 90
[12] Zhang K and Main P 1990 *Acta Cryst. A* **46** 41
[13] Xiang S, Carter C W Jr., Bricogne G and Gilmore C J 1993 *Acta Cryst. D* **49** 193
[14] Terwilliger T 2000 *Acta Cryst. D* **56** 965
[15] He Y, Yao D Q, Gu Y X, Lin Z J, Zheng C D and Fan H F 2007 *Acta Cryst. D* **63** 793
[16] Fan H F and Gu Y X 1985 *Acta Cryst. A* **41** 280
[17] Cowtan K D and Main P 1996 *Acta Cryst. D* **52** 43
[18] Terwilliger T C, Grosse-Kunstleve R W, Afonine P V, Moriarty N W, Zwart P H, Hung L W, Read R J and Adams P D 2008 *Acta Cryst. D* **64** 61
[19] Cowtan K 2012 *Acta Cryst. D* **68** 328
[20] Brohawn S G, del Mármol J and MacKinnon R 2012 *Science* **335** 436
[21] Yuan P, Leonetti M D, Pico A R, Hsiung Y and MacKinnon R 2010 *Science* **329** 182
[22] Chang W R, Jiang T, Wan Z L, Zhang J P, Yang Z X and Liang D C 1996 *J. Molecular Biology* **262** 721
[23] DeLano W L 2002 http://www.pymol.org [2019-05-20]
[24] Emsley P, Lohkamp B, Scott W G and Cowtan K 2010 *Acta Cryst. D* **66** 486
[25] Terwilliger T C 2000 *Acta Cryst. D* **56** 965